An Experimental Analysis to Assess Photo-Acoustic Techniques for Silver Nano-Particles; Considering Physical Properties

F. M. Aldosari[1], A. M. Azzeer[2], & A. M. Hassib[2]

[1] Prince Sattam Bin Abdulaziz University, Physics Department, Applied and Natural Sciences, Riyadh, Saudi Arabia

[2] Physics and Astronomy Department, College of Science, King Saud University, Riyadh, Saudi Arabia

Correspondence: F. M. Aldosari, Prince Sattam Bin Abdulaziz University, Physics Department, Applied and Natural Sciences, P.O. Box 380549, Riyadh 11345, Saudi Arabia. Tel: 966-11-682-6600. Fax: 966-11-682-6194. E-mail: fah.aldosari@psau.edu.sa

Abstract

Aim: To assess the photo-acoustic techniques for the calculation of size, distribution, shape and phase of silver nanoparticles. **Methodology:** The silver nanoparticles were synthesized by sodium borohydride ($NaBH_4$) and silver nitrate ($AgNO_3$). Nine samples were prepared with varying concentrations and the changes in their properties were studied. **Results:** The shape of the silver nanoparticles was found to be spherical in shape. The average size of the silver nanoparticles was calculated to be 4-27nm. The results suggested that the particle size was decreasing with increase in the concentration of the silver nanoparticles. The strongest peak was obtained at 392nm which corresponds to the concentration C1. The absorption peak was found to be shifting towards the longer waves with the decrease in concentration. The XRD analysis revealed that the silver nanoparticles corresponding to all concentrations possessed crystal cubic structure. **Conclusion:** The silver nanoparticles were being extensively used in various applications due to their unique physical properties.

Keywords: Photo-acoustic Techniques, Physical Properties, Silver Nano-particles, XRD Analysis

1. Introduction

Alexander Graham Bell discovered the photoacoustic effect in 1880 during his search for a wireless communication (Manohar & Razansky, 2016). Photoacoustic spectroscopy is widely used in several applications; thus, the photoacoustic spectroscopy is classified as a branch of photothermal technique. In this technique, the light beam is incident on the sample, which causes changes in the thermal state in the physical properties of the sample. The general theory behind photoacoustic technique is that, when the matter is irradiated with a certain frequency, which matches the resonant frequency of the matter; then some of the energy is absorbed in the matter causing excitement in the matter (Lum et al., 2018). As a result, the heat energy of the molecules is also increased thus, affecting several properties of the matter such as, pressure and temperature (Sandler, 2017).

There are four photoacoustic techniques, which can be used to study the physical properties of nanoparticles. The techniques are direct, indirect, continuous-wave and pulse modulation mode. The current study demonstrates the use of these techniques in various applications and for the identification of various physical properties. Thus, these techniques can be utilized to find the accurate physical properties of the silver nanoparticles. Silver nanoparticles have applications in various fields due to its small size and to identify associated parameters, which can help in increasing applications of silver nanoparticles.

1.1 Direct Photoacoustic Technique

In this technique, the optical absorption is not too high and a fraction of the incident light penetrates into the sample. The absorption of the portion forms an acoustic wave into the sample (Belhachmi, Glatz, & Scherzer, 2016). The technique is extremely useful in identifying the structure and internal composition of the sample. The sample is not enclosed into a volume which is of concern in most of the practical applications. The piezoelectric effect is the most well-known method of direct photoacoustic generation. The direct photoacoustic technique gives extremely high sensitivity during the measurement of the absorption coefficient. The piezo electric effect is produced by the accumulation of charges in specific areas due to mechanical stress (Cremer et al., 2017).

1.2 Indirect Photoacoustic Technique

In this technique, an acoustic wave is generated in a coupling medium adjacent to the sample. The coupling medium is either a gas or a liquid due to which the technique usually requires a closed photoacoustic cell. However, there are some actors, which influence the working of this technique and includes the limitations in case of a condensed matter (Zelewski & Kudrawiec, 2017). For example, heat transfer process from condensed matter to gas, low pressure limitations, and narrow bandwidth are associated with microphone responses. The following technique is less sensitive as compared to the direct technique; however, the technique is useful in the study of highly absorbent and opaque samples, which restrict the light passage (Sharma et al., 2017).

1.3 Continuous-Wave Modulation Mode

The continuous-wave modulation mode involves the duty cycle of the modulated beam and utilizes only 50% of the modulated cycle. Due to large amount of duty cycle, there are several effects such as boundary conditions of the acoustic cell, heating of the sample and the convection currents are of huge importance for the production of photoacoustic response (Beha et al., 2015). The continuous-wave modulation mode is not beneficial for several applications due to its boundary condition dependence. Moreover, this technique has other limitations such as the presence of apparent thermal diffusion, which lowers the photoacoustic sensitivity and competency. Therefore, this technique cannot be used in the diagnosis tasks and biomedical photoacoustic imaging (Devi, Kumar, & Ebrahim-Zadeh, 2015).

1.4 Pulsed Modulation Mode

This technique uses a high power and low duty cycle optical source for the production of photoacoustic wave. The photoacoustic competency and the thermal diffusion effects can be eliminated in this technique as the optical energy enters the sample in a short time interval. Other issues, such as, sample heating and convection currents can also be reduced in this technique. Thus, the technique is beneficial for various applications due to less limitations as compared to continuous-wave modulation mode. Mostly, pulse excitation mode is being used in all the modern photoacoustic techniques (Giorgianni et al., 2018).

2. Method

The materials used in this study for the synthesis of silver nanoparticles include sodium borohydride ($NaBH_4$) and silver nitrate ($AgNO_3$).

2.1 Synthesis of AuNPs

The $NaBH_4$ is used in an excess amount for the stabilization of the AuNPs and for reducing the ionic silver and the concentration of sodium borohydride was kept twice that of silver nitrate i.e. $[NaBH_4]/[AgNO_3] = 2.0$. The product breakdown occurred when sodium borohydride was varied from 2.0mM and the silver nitrate was kept at 1.0mM.

2.2 Experimental Setup

The experimental setup of the study included the Nd: YAG laser which has the following specifications: Rod diameter of 8mM; 532nm Polarization: horizontal; 1 mrad of beam divergence; 12ns pulse width at 532nm; 1-10Hz pulse repetition rate; 280mJ of pulse energy at 532nm; 532nm of output energy; pump energy of 23J, and 154 micro seconds of delay of out pulse related to pump pulse. Moreover, the experimental setup included a titanium-doped sapphire laser to study the relationship between wavelength and photoacoustic signal. The spectra of UV-VIS absorption of the silver nanoparticles was obtained with the help of UV-Visible spectrophotometer. The wavelength of the spectrophotometer was between the range of 190nm to 1100nm. Furthermore, mirrors were used in the experimental setup for the reflection of the radiation. Moreover, a holographic grating was being used in the monochromator. Halogen and deuterium lamp were being used as radiative sources. A suitable optical filter is being used in the path of the beam for the filtration of the radiation. The synchronous fluorescence, excitation and emission were obtained with the help of Luminescence Spectrometer. The source used for excitation was xenon flash lamp. To increase the photoacoustic signal, the photodiode amplifier was being used. To obtain the proper accurate shape of the electrical signal from the photodiode, the two-channel digital real-time oscilloscope was used. Moreover, an intensified charge coupled device was used to record the enhanced response. The Microtrac S3500 Tri-laser particle size analyzer was used for the measurement of the size of the particle. The particle size, distribution and the shape were obtained with the help of transmission electron microscopy. Lastly, X-ray diffraction was utilized for the analysis of quantification and phase. Moreover, the structure of the particle was also determined using High Score.

2.3 The Calibration

The Rhodamine 6G dye was used for the calibration of the experimental setup.

3. Results

The physical properties of silver nanoparticles, namely; shape, size, distribution, and phase were analyzed with the help of various techniques. UV-Spectrophotometer, Transmission Electron Microscopy, Microtrac S3500 Tri-laser particle size analyzer, and X-ray diffraction was carried out on the particles.

3.1 UV-Vis Spectrophotometer

The samples of silver nanoparticles consisting of different concentrations were analyzed with the help of UV-Vis Spectrophotometer. The concentrations were as followed:

$$C0 = 2.5 * 10^{-3} M$$
$$C1 = 1.25 * 10^{-3} M$$
$$C2 = 6.25 * 10^{-4} M$$
$$C3 = 3.125 * 10^{-4} M$$
$$C4 = 1.56 * 10^{-4} M$$
$$C5 = 7.81 * 10^{-5} M$$
$$C6 = 3.9 * 10^{-5} M$$
$$C7 = 1.95 * 10^{-5} M$$
$$C8 = 9.76 * 10^{-6} M$$

These samples were prepared for 2880 min and the spectrum was recorded for these samples using UV-Vis spectrophotometer. Moreover, the absorbance of sodium borohydride ($NaBH_4$), silver nanoparticles (Ag), and silver nitrate ($AgNO_3$) was also obtained with the help of UV-Vis spectrophotometer.

The strongest peak was obtained at 392nm corresponding to the concentration of C1. As the concentration was decreasing, the absorption was shifting towards longer waves.

Table 1. The obtained wavelength for the absorption of silver nanoparticles for varying concentrations

Time	λ	λ	λ	λ	λ	λ	λ	λ
(min)	(nm)	(nm)	(nm)	(nm)	(nm)	(nm)	(nm)	(nm)
	C1	C2	C3	C4	C5	C6	C7	C8
1440	392	392	390	390	392	394	382	382
2880	392	392	392	392	394	397	398	398
4320	392	392	392	392	394	398	388	386
5760	392	392	392	392	396	398	388	388
7200	394	392	392	392	396	398	388	392
8640	394	394	392	392	396	398	388	388
10080	394	392	392	392	396	398	388	390
20160	394	394	392	394	398	400	388	394
30240	394	394	392	396	398	400	388	398
40320	394	394	392	396	400	400	388	396
50400	394	394	392	396	400	400	388	400
60480	394	394	392	396	400	400	388	404
70560	392	394	392	398	400	400	390	402
80640	394	394	394	398	400	400	388	398

The data collected for the initial two weeks showed no difference in the symmetry and the position of absorption peaks. However, the data collected after 4 weeks showed a slight red shift from 392nm to 400nm; thus, forming particles of relatively larger size without aggregation. No aggregation and Plasmon absorbance were observed even after 2 months; thus, suggesting the stability of colloidal silver at room temperature for months or weeks.
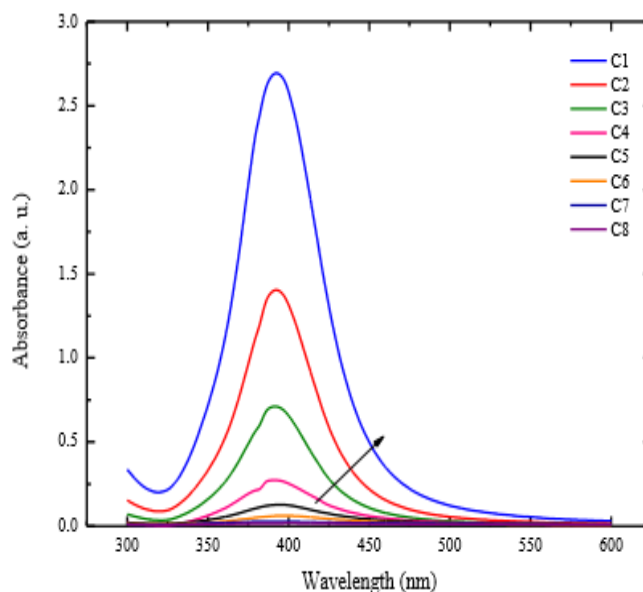
Figure 1. The spectra of silver nanoparticles with different concentrations after 2880 min using UV-Vis spectrophotometry

3.2 Transmission Electron Microscopy

TEM analysis was carried out on the silver nanoparticles to study the morphology and size of the particles with varying concentrations from C0 to C5. By evaluating the results obtained from the TEM analysis, it was concluded that the silver nanoparticles have spherical shape. The diameter of the silver nanoparticles was calculated to be 2-40nm.
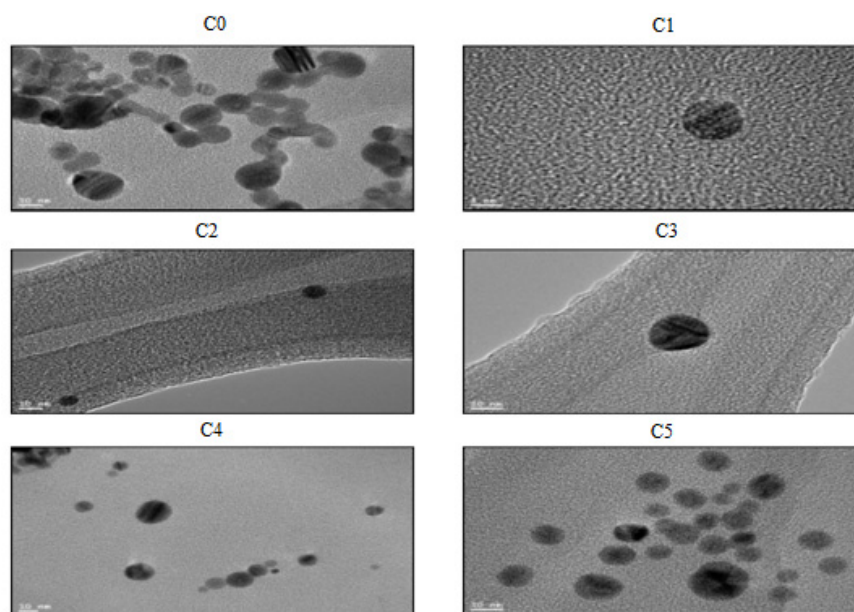

Figure 2. TEM images of silver nanoparticles in water with concentrations: C0, C1, C2, C3, C4, C5

The TEM images of the silver nanoparticles of concentration C6, C7, and C8 were found to be different than other concentrations. The spectrum also showed different results as compared to the concentrations from C0 to C5. The TEM images shows that the silver nanoparticles corresponding to C6, C7, C8 were aggregated.
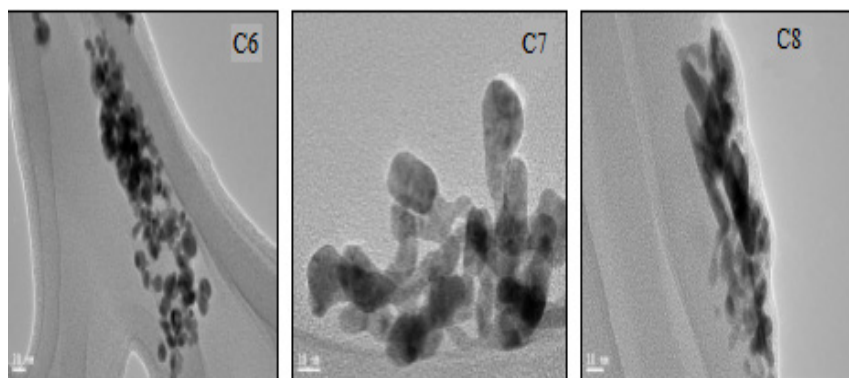
Figure 3. Aggregated TEM images of silver nanoparticles in concentrations C6, C7, and C8

3.3 Microtrac S3500 Particle Size Analyzer

The results obtained from the Microtrac particle size analyzer provided the size measurement of the silver nanoparticles corresponding to different concentrations. The results obtained showed an inverse relationship between the particle size and the concentration i.e. when the concentration was increased, the size of the particle was decreased. The average size of the nanoparticles was found out to be 4-27nm. Figure 4 shows the relationship between the size and the concentration of the silver nanoparticles. Figure 5 shows the results obtained with the help of Microtrac for different concentrations.
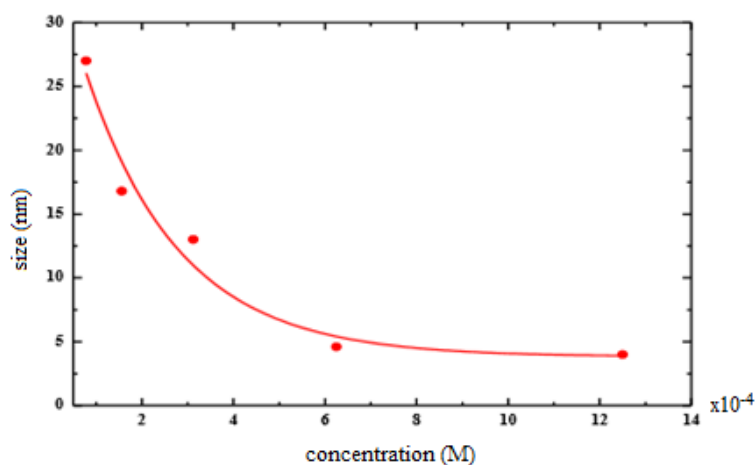

Figure 4. Size (diameter) vs. concentration from Microtrac after 2880 min

3.4 X-Ray Diffraction (XRD) Analysis

XRD analysis was carried out on the samples with varying concentrations for phase analysis and crystal structure's quantification. The XRD patterns revealed that the silver nanoparticles corresponding to all concentrations possessed cubic crystal structure. The peaks were obtained at $2\theta=38.48°$, $44.67°$, $82.4°$ and $98.99°$ and the crystal faces corresponding to each peak were found out to be 111, 200, 222 and 400. The results of the XRD patterns showed that the crystalline structure of the heat silver nanoparticles was not disturbed by the silver nanoparticles. Face-centered cubic (FCC) silver was indexed from the reflection peaks obtained from the XRD patterns. The particle size of the silver nanoparticles was calculated with the help of the Scherrer equation, in regards with the full width at half maximum of the diffraction peaks. The resulting particle size was calculated to be 39, 51, 27 and 21nm. The average size calculated from the XRD pattern corresponding to the silver nanoparticles was 34.5nm. The XRD results were found to be consistent with the TEM images (Figure 6).

$$Dn = \frac{K\lambda}{(\beta cos\theta)} \tag{1}$$

Here, λ is the wavelength of the X-ray and is equal to 1.54nm, K is the Scherrer's constant and is equal to unity, θ is the diffraction angle, and β is the full width of maximum height of a diffraction peak.
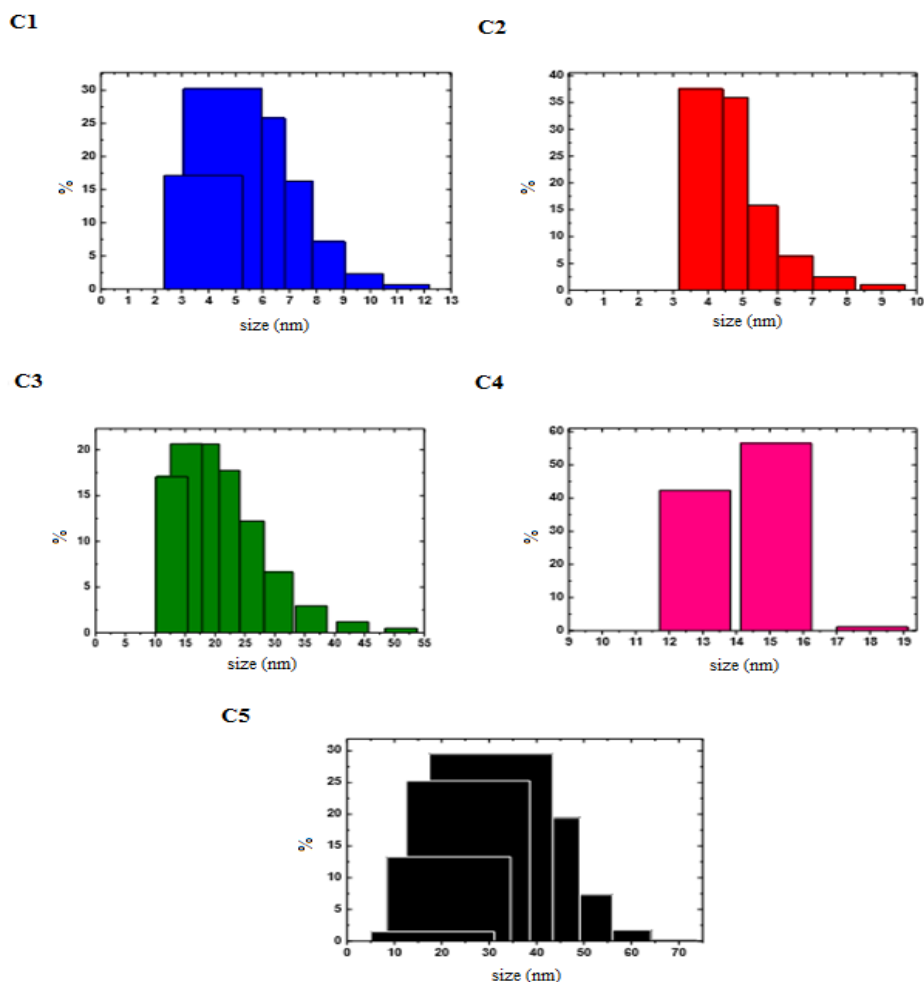
Figure 5. Histogram representation of the nanoparticles for C1, C2, C3, C4, C5 concentrations
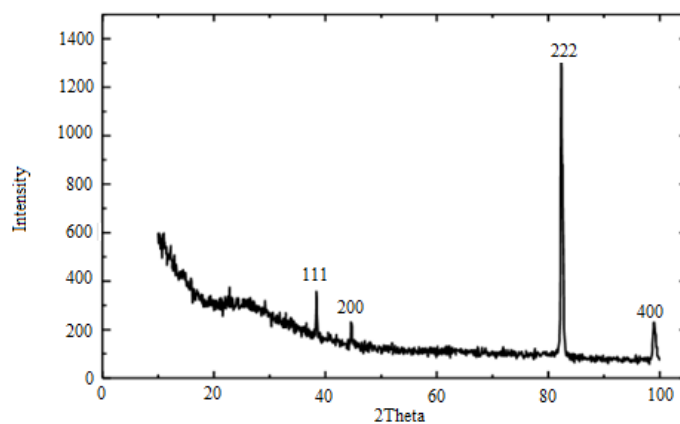
Figure 6. XRD pattern of silver nanoparticles

XRD pattern is used for structural analysis and is a canonical technique. However, XRD cannot be used to analyze nanoparticles, because nanoparticles do not have good X-ray scattering sources. The nanoparticles possess a number of displacement and structural disorder. Furthermore, XRD do not measure the absolute structural properties of the nanoparticles since it averages over atomic distances. Due to non-crystalline structures within the sample and overlapping peaks, Scherrer formula can be applied to the samples of nanoparticles. The XRD analysis obtained are not accurate for 100nm particles in size; therefore, only the measurements collected through the Microtrac S3500 will be considered.

4. Discussion

The study aimed to assess the photo-acoustic techniques for measuring the physical properties of silver nanoparticles. The results obtained from UV-Spectrophotometer indicated that the strongest peak obtained at 392nm that corresponded to the concentration of C1. Moreover, an absorption shift was noted towards the longer waves as the concentration was decreasing. These findings have been corroborated by previous studies. For instance, Vanaja et al. (2013) conducted UV-Spectrophotometer analysis whose results were found to be consistent with current study. Due to the change of color of the solution, the presence of silver nanoparticles was confirmed. The physical and chemical properties of the silver nanoparticles obtained from the study were found to be dependent upon factors; such as, incubation time, temperature, pH, and metal ion concentration. The study showed that while increasing the concentration of the silver nanoparticles, their formation was increased. Due to an increase in the concentration of silver nanoparticles from 1mM concentration, the band shifted from 410nm to 450 nm.

Another study conducted by Koyyati et al. (2014) used UV- Vis spectrophotometer to confirm the formation of silver nanoparticles. The use of nano biotechnology is emerging as an important branch of nanotechnology. In the study, the UV-Vis absorption was evaluated after re-dispersing and centrifuging the particles in the deionized water. The absorption peak of the particles was obtained at 423.5nm. Moreover, SEM analysis were also carried out on the silver nanoparticles, which confirmed the particle size to be around 5-20nm and the shape of the particles to be spherical. The shape of the silver nanoparticles was also found to be spherical in the current study as calculated with the help of TEM analysis.

In addition, the results obtained from TEM showed that the images obtained for the samples from C0 to C5 suggested that the silver nanoparticles were spherical in shape and their diameter was calculated to be 2-40nm. The TEM images obtained for the samples C6-C8 showed different results as compared to the samples from C0-C5. Moreover, the samples were found to be aggregated. TEM is an advanced, powerful and fast-growing technique for the assessment of chemistry and structure of the nanoparticles with accuracy (Su, 2017). TEM analysis are extensively carried out in various studies to evaluate the structure of the nanoparticles and to evaluate their implications in various fields of technology.

A study conducted by Sathyavathi et al. (2010) conducted an experiment for the biosynthesis of silver nanoparticles using Coriandrum Sativum leaf extract. The characteristics of the silver nanoparticles were characterized with the help of XRD, UV-Visible, FT-IR, and TEM. The results obtained from UV-Visible spectroscopy showed that the absorption spectrum of the silver nanoparticles shifted from 440nm to 427nm. Moreover, the XRD analysis showed that the structure of the silver nanoparticles was found out to be cubic crystal structure, as predicted in the current study. Furthermore, the TEM analysis of the silver nanoparticles showed that the silver nanoparticles were found to be spherical in shape, which was found to be consistent with the present study findings.

The results obtained from the particle size showed a reduction in the concentration. The particle size was decreasing as the concentration of the sample was increased. The particle size plays an important role in determining the applications of the nanoparticles. A study conducted by Akbari, Tavandashti and Zandrahimi (2011) evaluated the particle size characterization of nanoparticles. The particle size and the size distribution of alumina nanoparticles were evaluated in the following study. The particle size was determined by carrying out TEM, PCS, BET, and XRD peak broadening analysis. The particle size of alumina nanoparticles was found out to be 5-95nm. Thus, the particle size plays a critical role in determining the properties of a particular nanoparticle.

In the end, XRD analysis were carried out on the samples for phase analysis. The structure of the silver nanoparticles as suggested from this technique showed that the silver nanoparticles corresponding to all concentrations was found to be cubic crystal structure. The XRD results were found to be consistent with the results obtained from TEM imaging. Moreover, the average particle size was calculated to be 34.5nm. Ganesan et al. (2014) conducted a study to analyze the bioinspired synthesis of silver nanoparticles using the leaves of Millngtonia hortensis. The XRD analysis were carried out on the silver nanoparticles to study their structure and the results obtained showed that the silver nanoparticles were mostly crystalline in nature. The calculated size of the particles was found out to be in the size range of 20nm to 64nm and the average size was found out to be 44nm.

The physical properties calculated in the study were the size, shape, distribution, and phase of the silver nanoparticles. The physical properties were assessed by using UV-Vis Spectrophotometer, Transmission Electron Microscopy (TEM), Microtrac particle size analyzer, and XRD. The study showed that the shape of the silver nanoparticles was spherical and the particles were crystalline in nature. The diameter of the silver nanoparticles was calculated to be 2-40nm. The study showed that the particle size of the silver nanoparticles was decreasing

with the increase in concentration and the absorption spectrum was shifting towards longer waves as the concentration was decreasing. It can be concluded from the study that due to unique properties of silver nanoparticles; they are being extensively used in biotechnology, electrical, optical, and chemical sensors. Future studies should focus more on the silver nanoparticles effect size by undertaking additional particle size and phases.

Acknowledgement

References

Akbari, B., Tavandashti, M. P., & Zandrahimi, M. (2011). Particle size characterization of nanoparticles-a practicalapproach. *Iranian Journal of Materials Science and Engineering, 8*(2), 48-56.

Beha, K., Cole, D. C., Del'Haye, P., Coillet, A., …, & Papp, S. B. (2015). Self-referencing a continuous-wave laser with electro-optic modulation. *arXiv preprint*.

Belhachmi, Z., Glatz, T., & Scherzer, O. (2016). A direct method for photoacoustic tomography with inhomogeneous sound speed. *Inverse Problems, 32*(4), 045005.

Cremer, J. W., Covert, P. A., Parmentier, E. A., & Signorell, R. (2017). Direct measurement of photoacoustic signal sensitivity to aerosol particle size. *The Journal of Physical Chemistry Letters, 8*(14), 3398-3403.

Devi, K., Kumar, S. C., & Ebrahim-Zadeh, M. (2015). Phase-modulation-mode-locked continuous-wave MgO: PPLN optical parametric oscillator. *IEEE Photonics Journal, 7*(2), 1-8.

Friedrich, K., & Breuer, U. (2015). *Multifunctionality of polymer composites: Challenges and new solutions*. William Andrew.

Ganesan, V., Deepa, B., Nima, P., & Astalakshmi, A. (2014). Bioinspired synthesis of silver nanoparticles using leaves of Millngtonia hortensis L. F. *Int. J. Adv. Biotechnol. Res, 5*, 93-100.

Giorgianni, F., Vicario, C., Shalaby, M., Tenuzzo, L. D., ... & Lupi, S. (2018). High-Efficiency and Low Distortion Photoacoustic Effect in 3D Graphene Sponge. *Advanced Functional Materials, 28*(2), 1702652.

Koyyati, R., babu Nagati, V., Nalvothula, R., Merugu, R., …, & Padigya, P. R. M. (2014). Antibacterial activity of silver nanoparticles synthesized using Amaranthus viridis twig extract. *International Journal of Research in Pharmaceutical Sciences, 5*(1), 32-39.

Lum, J. S., Stobbe, D. M., Borden, M. A., & Murray, T. W. (2018). Photoacoustic technique to measure temperature effects on microbubble viscoelastic properties. *Applied Physics Letters, 112*(11), 111905.

Manohar, S., & Razansky, D. (2016). Photoacoustics: A historical review. *Advances in Optics and Photonics, 8*(4), 586-617.

Sandler, S. I. (2017). *Chemical, Biochemical, and Engineering Thermodynamics*. John Wiley & Sons.

Sathyavathi, R., Krishna, M. B., Rao, S. V., Saritha, R., & Rao, D. N. (2010). Biosynthesis of silver nanoparticles using Coriandrum sativum leaf extract and their application in nonlinear optics. *Advanced Science Letters, 3*(2), 138-143.

Sharma, R. C., Kumar, S., Gautam, S., Gupta, S., & Srivastava, H. B. (2017). Photoacoustic sensor for trace detection of post-blast explosive and hazardous molecules. *Sensors and Actuators B: Chemical, 243*, 59-63.

Su, D. (2017). Advanced electron microscopy characterization of nanomaterials for catalysis. *Green Energy & Environment, 2*(2), 70-83.

Vanaja, M., Gnanajobitha, G., Paulkumar, K., Rajeshkumar, S., …, & Annadurai, G. (2013). Phytosynthesis of silver nanoparticles by Cissus quadrangularis: Influence of physicochemical factors. *Journal of Nanostructure in Chemistry, 3*(1), 17.

Zelewski, S. J., & Kudrawiec, R. (2017). Photoacoustic and modulated reflectance studies of indirect and direct band gap in van der Waals crystals. *Scientific Reports, 7*(1), 15365.

Copyrights